

## **Cu and Co modified beta zeolite catalysts for the trichloroethylene oxidation**

N. Blanch-Raga<sup>+</sup>, A.E. Palomares\*, J. Martínez-Triguero, S. Valencia  
*Instituto de Tecnología Química, UPV-CSIC, Valencia, 46022, Spain*

<sup>+</sup> *in leave to departament of Biobased Commodity Chemicals, Wageningen University (The Netherlands)*

\* Corresponding author:

Antonio Eduardo Palomares

E-mail address: [apalomar@iqn.upv.es](mailto:apalomar@iqn.upv.es)

Instituto de Tecnología Química, UPV-CSIC,

Universitat Politècnica de València

Camino de Vera s.n. 46022 Valencia (Spain)

(+34) 96 387 7007 (ext. 76377)

## **ABSTRACT**

In this work we have studied for the first time the catalytic activity for the oxidation of trichloroethylene (TCE) of Cu and Co beta zeolites. The results show that they are active and selective towards CO<sub>2</sub>, obtaining a better selectivity than that reached with conventional H-zeolites. The copper and cobalt zeolites have been prepared by different methods. It was found that their activity depend on the metal and on the preparation procedure. The most active catalyst was the Cu-BEA prepared by ion exchange ( $T_{50\%} = 310^{\circ}\text{C}$  and  $T_{90\%} = 360^{\circ}\text{C}$ ). This catalyst has the highest ammonia adsorption capacity (as a measurement of the acidity) and it was the only tested material in which the  $\text{Me}^{2+}$  was completely reduced in a standard H<sub>2</sub>-TPR experiment (indicative of its important redox properties). Thus, the enhanced activity of the Cu-exchanged zeolite was associated to the presence of strong acid sites in the zeolite and to the redox properties of the copper ion exchanged. The catalyst was stable at 300°C for almost 70 hours without any important deactivation. This was related to the oxidative properties of the copper that avoid the formation of coke on the strong acid sites of the zeolite. On the other hand, zeolites with the transition metal incorporated into the zeolite framework by hydrothermal synthesis showed lower catalytic activity, probably because the formation of small oxide particles with much less interaction with the silicate framework, that results in a lower redox activity of the transition metals. It has been shown that a proper combination of acidity, redox properties and metal-zeolite interaction is necessary in order to prepare an active and selective zeolite catalyst for the TCE oxidation.

## **KEYWORDS**

Catalytic oxidation, chlorinated VOCs, trichloroethylene, zeolite beta, copper, cobalt.

## 1. INTRODUCTION

Volatile organic compounds (VOCs) are defined as any organic compound having at 293.15 K, a vapor pressure of 0.01 kPa or more, or having a corresponding volatility under the particular conditions of use (Council Directive 1999/13/EC of 11<sup>th</sup> March 1999). They are widespread applied in industry, mainly as solvents. Nevertheless, VOCs are considered as pollutants because their toxicity and their contribution to the formation of low-level ozone (photochemical smog) and to the ozone layer depletion (mainly the CFC). Trichloroethylene (TCE) is a common chlorinated VOC that was a dominant cleaning product in the 70's and now is commonly used for the degreasing of mechanical parts and dry-cleaning [1]. It has been classified as probably carcinogenic to humans by the International Agency for Research on Cancer [2]. For these reasons the control of the TCE emissions is an important issue for environmental protection.

Thermal incineration has become the conventional method of reducing VOC emissions from industrial processes. It has proved to be successful in many processes but it has major drawbacks [3]. First, temperatures must reach over 1000°C for the complete pollutant destruction making it an uneconomical process. In addition the high temperatures reached in this process generate higher quantities of NO<sub>x</sub> and finally, this technique is not very effective with low pollutant concentration streams.

Catalytic oxidation of VOCs is a realistic contender to the conventional method [4, 5]. It requires lower temperatures (250-550°C), generating less energetic costs and preventing the formation of non-desired by-products. Several catalysts, as metal oxides [6-11], bronzes [12] and noble metals supported on different materials [13] have been studied for the catalytic oxidation of chlorinated organic volatile compounds (CVOCs), but they have problems related with the catalyst deactivation and with the formation of toxic by-products [14]. Other materials, as acid zeolites have been described as alternative catalysts for the trichloroethylene oxidation [15]. However, after a certain period of time, acid zeolites deactivate due to coke deposition and chlorine attack to the acid sites [16]. In these catalysts, Brönsted acidity plays an important role, controlling the oxidative activity of the zeolites [15, 17]. It was found [17, 18] that dealumination of Y zeolite by ammonium hexafluorosilicate was a procedure that can improve the catalytic activity of H-Y zeolites for chlorinated VOC decomposition, due to the strong Brönsted sites formed in the dealumination treatment.

Other strategies were based in a combination of transition metals and zeolites [19-21]. In this way, Divakar *et al.* [22] studied the catalytic activity of ZSM-5 and Beta zeolites with Fe and they found that all the catalysts were active for the trichloroethylene oxidation, but the results obtained depended on the catalyst preparation procedure. Huang *et al.* [23] studied the synergy between

Cr<sub>2</sub>O<sub>3</sub>-CeO<sub>2</sub> and USY zeolite on the catalytic performance, showing that the interaction between chromium and cerium improves the mobility of oxygen species, favouring the oxidation of the chlorinated volatile organic compounds. These results show that the interaction of the transition metal and the zeolite improves the catalytic activity of the material. This interaction depends on the way the transition metal is incorporated to the zeolite structure and this has never been previously studied for this reaction. In this work we have studied this topic by using different catalysts based on beta zeolites for the TCE oxidation.

Beta zeolite was chosen because it can be synthesized with a wide range of Si/Al molar ratios and other elements different from Si and Al can be incorporated to the material. It is the only high-silica zeolite possessing a three-dimensional intersecting channel system of large pores with high thermal and hydrothermal stability, high diffusion capacity and low steric restrictions, assuring the absence of diffusional limitations. In addition, transition metals can be added to the zeolite by different post-synthesis methods (as ion exchange, incipient wetness impregnation, etc.) or they can be integrated in the zeolite framework during the synthesis process. Some papers have reported [24-27] the high activity of the latter zeolites in different redox reactions. Thus, it could be expected that these catalysts are also active for the TCE oxidation. Furthermore, by comparing the activity of zeolites with transition metals incorporated by different processes, we can study the influence of the metal-zeolite interaction in the catalyst behaviour. In this paper, Cu and Co zeolites have been prepared by ion exchange and by hydrothermal synthesis and the catalytic activity of these materials for the TCE oxidation reaction has been studied and compared with that of H-BEA zeolite.

## **2. MATERIALS AND METHODS**

### **2.1. Catalysts preparation**

A commercial acid beta zeolite (CP811, PQ Zeolites B.V.) was used as a reference material. Some catalysts were prepared from this parent material by adding copper or cobalt to the zeolite by a conventional ion-exchange procedure. The metal exchange was performed in an aqueous solution containing Co(CH<sub>3</sub>COO)<sub>2</sub>·4H<sub>2</sub>O or Cu(NO<sub>3</sub>)<sub>2</sub>·6H<sub>2</sub>O with the adequate concentration to achieve the desired amount of metal on the zeolite and with a solid/liquid ratio of 1/150. The metal exchange was at 80°C for the Co-samples and at room temperature for the Cu-samples. After 24 h under mechanical stirring, the solutions were washed, filtered and dried at 100°C [28]. In the case of the Cu-sample, before washing, a 0.1 M NH<sub>4</sub><sup>+</sup> solution was added to increase the pH of the solution up to 6-7. After drying the samples, they were heat-treated at 450°C for 4 h.

In other group of catalysts, copper or cobalt were added to the zeolite framework by hydrothermal synthesis. In order to prepare the catalysts, a procedure based on that published in reference [29] was followed. In particular, tetraethylorthosilicate (TEOS, Merck) was hydrolysed in an aqueous solution of tetraethyl ammonium hydroxide (TEAOH, 35%, Aldrich). Then,  $\text{Cu}(\text{NO}_3)_2 \cdot 6\text{H}_2\text{O}$  or  $\text{Co}(\text{NO}_3)_2 \cdot 6\text{H}_2\text{O}$  (Aldrich) dissolved in deionized water was added and the mixture was stirred at room temperature in order to evaporate the ethanol produced during the hydrolysis of TEOS. After that, HF was added to the mixture and finally a suspension of zeolite beta seeds in water was added. The final gel composition was:



where MeO represents the metal (Cu or Co) expressed as the corresponding oxide.

The solid obtained was transferred to a Teflon-lined stainless-steel autoclave and heated up to  $140^\circ\text{C}$  while being rotated at 60 rpm. After 7 days at the crystallization temperature, the autoclave was quenched, the content filtered and the solid washed with deionized water, dried at  $100^\circ\text{C}$  and calcined at  $580^\circ\text{C}$  for 3 h.

All catalysts were pelletized, and then the pellets were crushed and sieved to obtain grains of 0.25-0.45 mm in diameter. Materials were named as beta-Cu (X) or beta-Co (X), where X corresponds to the preparation method of the samples, i.e. IE (ion exchange) and HS (hydrothermal synthesis).

## 2.2. Catalysts characterization

The surface areas of the different catalysts were measured on an ASAP 2010 instrument (Micromeritics) using the BET method from the nitrogen adsorption isotherms at  $-196^\circ\text{C}$ .

Powder X-ray diffraction patterns (XRD) were collected using an X'Pert-Pro diffractometer (Panalytical) equipped with an X'Celerator detector and using Ni-filtered  $\text{Cu K}\alpha$  radiation.

The chemical composition of the samples was measured by inductively coupled plasma (ICP-OES) in a Varian 715-ES ICP-Optical Emission Spectrometer.

Temperature programmed reduction (TPR) experiments were carried out using a TPD-TPR Autochem 2910 analyzer equipped with a thermal conductivity detector. The reduction of the samples (10-20 mg) was conducted from 25 to  $800^\circ\text{C}$  with a thermal ramp of  $10^\circ\text{C} \cdot \text{min}^{-1}$  using a  $\text{N}_2:\text{H}_2$  flow (10%  $\text{H}_2$ ) of  $50 \text{ mL} \cdot \text{min}^{-1}$ .

Temperature programmed desorption of ammonia (TPD) experiments were carried out in a Micromeritics Autochem II analyzer. Before the adsorption, 300 mg of the sample was pre-treated with Ar at  $450^\circ\text{C}$  for 1 h and then it was cooled down to  $10^\circ\text{C}$ . Ammonia was chemisorbed by pulses at  $100^\circ\text{C}$  until equilibrium was reached, then the sample was flushed with He for 15 min. The desorption was carried out from 100 to  $500^\circ\text{C}$  with  $100 \text{ mL} \cdot \text{min}^{-1}$  of He and using a heating

rate of  $10^{\circ}\text{C}\cdot\text{min}^{-1}$ . The  $\text{NH}_3$  desorbed was monitored by both thermal conductivity detector and mass-spectrometry following the characteristic mass of ammonia at  $m/e = 15$ .

Transmission electron microscopy (TEM) images were obtained with a JEOL JEM-1010 microscopy, operating at 100 kV. Samples were prepared by suspending the solid in ethanol and with ultrasonic treatment for 30 minutes. Then, a drop of the solution was deposited on a copper grid (300 mesh) covered by a perforated layer of carbon.

### 2.3. Catalysts activity

The catalytic tests have been performed in a quartz fixed bed reactor. The desired mass of the catalyst (0.68 g) was placed on a quartz plug located inside the reactor. Crushed quartz was placed above the catalyst as a preheating zone. The temperature was measured with a K-thermocouple located inside the reactor and the reactor was heated using an electrical oven. The flow rate was set at  $400\text{ ml min}^{-1}$  and the gas hourly space velocity (GHSV) was  $15000\text{ h}^{-1}$  at atmospheric pressure. The residence time, based on the packing volume of the catalyst, was 0.24 s. Liquid trichloroethylene was injected in an air flow with a syringe pump in order to have 1000 ppm of TCE in the gas flow. The reaction temperature was increased from 150 to  $550^{\circ}\text{C}$  in steps of  $50^{\circ}\text{C}$ . Each temperature was kept during 30 min before the analysis of the gas. The overall length of the reaction was six hours.

The organic compounds of the gas flow were analysed with a Bruker 450 gas chromatograph equipped with a HP-5 column and with a flame ionization detector.  $\text{CO}$  and  $\text{CO}_2$  were separated with micro-packed columns and analysed with a thermal conductivity detector.  $\text{Cl}_2$  and  $\text{HCl}$  were absorbed in a solution containing  $\text{NaOH}$  0.125M. The concentration of the absorbed  $\text{Cl}_2$  was determined by titration and the  $\text{HCl}$  concentration was measured using an ion selective electrode.

All experiments were repeated three times to assure the reproducibility of the results. In all the experiments the error analysis of triplicate results was under 5%.

## 3. RESULTS AND DISCUSSION

### 3.1. Catalysts characterization

**Figure 1** presents the XRD patterns of the zeolites studied in this paper. It can be seen that the diffractogram only shows the peaks associated to the crystal phase of a zeolite beta structure, i.e. with the main diffraction peaks at 7.2, 7.9, 12.5, 13.6, 21.4, 22.5, 25.4, 27.2, 28.8, 29.6 and  $33.6^{\circ}$  [29] and none of the samples contained any visible amorphous material. Zeolites with Cu or Co

prepared by hydrothermal synthesis also show the characteristic diffractogram of a zeolite beta structure but with much more defined peaks than the other zeolites. This was representative of a high crystallinity and it was related to the zeolite crystallite size, indicating that the crystallite size of the samples prepared by hydrothermal synthesis was much larger than that of the ion exchanged samples. It must be also pointed out that the zeolites prepared by hydrothermal synthesis were synthesized in a fluoride media leading to a low amount of silanol defects in the zeolite framework, then with a high peak resolution in the XRD patterns. On the other hand, no peaks associated to copper or cobalt oxides were observed in any sample, showing that copper and cobalt particles must be beyond the detection limit of the X-ray diffraction and thus, indicating a good metal dispersion on the catalyst surface [30].

**Table 1** shows the specific surface area, pore volume, pore size and the elemental composition of the samples. The zeolites prepared by hydrothermal synthesis have no aluminium in its composition due to the synthesis conditions necessary for their preparation [29]. The BET surface area of the samples was high and it varied between 440 and 590 m<sup>2</sup> g<sup>-1</sup>. The higher surface area corresponded to the parent zeolite and to the Cu and Co zeolites prepared by ion exchange. These zeolites have the same micropore volume and the same surface area than the parent zeolites. This indicates that the addition of the copper and cobalt do not block the zeolite pores and that the calcination of the samples after the ion exchange does not modify the zeolite structure. On the contrary, zeolites prepared by hydrothermal synthesis had a lower surface than the commercial zeolite. This can be related with the different crystallite size of the zeolites. As it was observed by XRD (**Figure 1**), the commercial zeolite had a smaller crystallite size and then a higher (interparticle) mesoporous volume. This led to a higher external surface area and consequently to a higher total surface area. On the other hand, the samples prepared by hydrothermal synthesis had a larger crystallite size, thus, a very small mesoporous volume. The total surface area of these samples was only associated with the microporosity resulting in lower values of surface area if compared to those of the zeolites prepared by ion exchange.

The different crystallite size was clearly observed by transmission electronic microscopy (TEM). As it can be seen in **Figure 2**, the zeolite prepared by ion exchange had an uniform particle size distribution and a round morphology with crystallites smaller than 50 nm, identical to the parent zeolite (not shown), indicating that the ion exchange had not modified the overall appearance of the zeolite at a microscopic level. In contrast, the micrograph of the zeolite prepared by hydrothermal synthesis exhibited a very different aspect. In this case, much larger crystallites were obtained with a crystallite size of approximately 1500 nm. The different crystallite size among both zeolites matched perfectly with the previous XRD results, confirming that the samples prepared by hydrothermal synthesis had a higher crystallinity because of their bigger crystallite size.

The NH<sub>3</sub>-TPD profiles of the zeolites were used to determine the number and strength of the acid sites present in the catalysts. The amount of desorbed ammonia was taken as a measure of the catalyst acidity, while the temperature in which ammonia was desorbed indicates the acid-strength distribution. The results are shown in **Figure 3** and **Table 2**. The most important feature was the difference in the ammonia desorption profiles between the zeolites prepared by hydrothermal synthesis and the samples prepared by ion exchange. As it can be seen, the acidity of the catalysts prepared by ion exchange (determined by the total area of the graph) was much higher than that of the samples prepared by hydrothermal synthesis. This can be related with the absence of aluminium in the latter zeolites and with the low acidity generated by copper or cobalt present in the HS-zeolites. On the contrary, the acidity of the ion exchanged catalysts was higher mainly due to the presence of H-sites corresponding to protons that were not fully exchanged with copper or cobalt. In both type of zeolites, Cu-samples adsorbed more ammonia than Co-samples.

As it can be seen in **Figure 3**, the catalysts showed a main desorption peak which could be split into two components, one centred around 180-200°C associated to weak acid sites (Lewis or Brönsted) and another centred around 275-300°C related to the presence of strong Brönsted acid sites [31]. The major component of the peaks corresponds to the first one, indicating the presence of weak acid sites in all the zeolites. The second component of the peak, representative of strong Brönsted acid sites, appears only in the ion-exchanged samples, especially in the beta-Cu (IE). Moreover another undefined peak was observed around 500-550°C in beta-Co (IE) and in beta-Cu (IE) that was related with the cationic metals exchanged in the zeolite. Thus, the results obtained showed an increase in the number and strength of the zeolite acid sites in this order: beta-Co(HS) < beta-Cu(HS) << beta-Co(IE) < beta-Cu (IE).

**Figure 4** presents the H<sub>2</sub>-TPR profiles of the zeolites tested. It can be seen that the Cu-exchanged sample had two reduction peaks around 190° and 450°C which could be assigned to the reduction of copper from Cu<sup>2+</sup> to Cu<sup>+</sup> (the lowest temperature peak) and then to the reduction from Cu<sup>+</sup> to Cu<sup>0</sup> [32]. The sample prepared with copper by hydrothermal synthesis presented both peaks but at different temperatures (225 and 280 °C) and with the relative intensities altered, probably due to the different interaction of the copper species with the zeolite matrix and to the different aluminium content [32, 33]. TPR results indicate that the monovalent state of copper ions is stabilized in Cu-beta zeolites, modifying the redox properties of the material and stabilizing the active sites. Nevertheless, the broadness and asymmetry of the first peak in the beta-Cu (HS), also suggests the presence in this sample of some Cu<sup>+2</sup> in dispersed undefined CuO species, that are reduced in one-step directly to Cu(0) [34].

Regarding the cobalt-containing samples, both of them presented a broad reduction peak between 550 and 750°C which could be attributed to the reduction of the cobalt atoms interacting with the



aluminium framework [7] or to the reduction of  $\text{Co}^{2-x}$  species [35]. It was observed that the beta-Co (HS) has a sharper and better defined peak than the beta-Co (IE), indicating the presence of more homogeneous cobalt species in this sample. These results could be related with the formation of different metal species as metal-oxo cations [36] that reduce in the range from 400 to 800°C. Nevertheless the formation, in a minor extent, of bare Co(II) ions balanced by the isolated Al atoms cannot be discarded [37].

The hydrogen consumption in the TPR measurements was quantified by integrating the area under the reduction peaks, in order to check if the reduction of the metal was complete at 800°C. These data are shown in **Table 3**. It was observed that the  $\text{H}_2/\text{Cu}$  ratio of the beta-Cu (IE) catalyst was  $\approx 1$  (considering experimental error), meaning that according to stoichiometry, all the  $\text{Cu}^{2+}$  was reduced to  $\text{Cu}^0$  in this catalyst. This did not occur with the other copper catalyst, where the  $\text{H}_2/\text{Cu}$  ratio was 0.33, indicating that only third part of the copper was completely reduced. On the other hand, in both Co-zeolites the  $\text{H}_2/\text{Co}$  ratio was  $< 1$  probably due to the presence of  $\text{Co}^{2-x}$  species [33] and/or to a strong interaction between the cobalt and the zeolite matrix preventing the complete reduction of the catalysts at 800°C.

These results also gave us some information about the state of the metals in the HS-zeolites. In principle, the incorporation of divalent atoms in framework positions would not provide redox properties to the materials if they are maintained in the framework after calcination, but acidic properties. As important acidic properties were not obtained with these zeolites (the TPD results shows the absence of strong acid sites), but some redox properties were observed (as the TPR results show), we can guess that the metals are not fully maintained in tetrahedrally coordinated framework positions. Probably, they have been partially extracted in the calcination procedure necessary to remove the organic template used for the zeolite synthesis. This results in an intermediate state where the metals are partially attached to the framework and some well dispersed clusters are formed with a small enough size to be undetectable by XRD or by high resolution electron microscopy [38]. These species do not adsorb basic molecules [37] as it was shown by the TPD results and they are forming some oxo-cationic species [39-40] as it was observed in the TPR experiments.

### 3.2. Catalytic activity results

The catalysts have been evaluated for the oxidation of trichloroethylene by monitoring the conversion as function of the temperature (light-off curve). **Figure 5** shows these results for a blank experiment, for a commercial acid beta zeolite (used as reference catalyst) and for the Cu and Co beta zeolites prepared by hydrothermal synthesis.

In absence of the catalyst (thermal oxidation) there was no conversion below 400°C. On the other hand, in the presence of the H-beta zeolite, the catalytic activity started at around 250°C and it rose up to 72% of TCE conversion at 550°C. The catalyst  $T_{50\%}$  (temperature at which 50% of the trichloroethylene conversion was reached) was around 410°C. The activity of the samples containing copper and cobalt, prepared by hydrothermal synthesis, was slightly better than that obtained with the H-zeolite, being the Cu-containing catalyst more active ( $T_{50\%} = 370^\circ\text{C}$ ) than the cobalt zeolite ( $T_{50\%} = 390^\circ\text{C}$ ). These results indicate that the addition of copper and cobalt to the zeolite framework by hydrothermal synthesis somewhat improves the activity of the reference H-beta material. In **Figure 6** are shown the results obtained with the ion exchanged beta zeolites and they are compared with those obtained with the H-zeolite and with a blank experiment. As it can be seen, the Co-exchanged zeolite had a similar activity ( $T_{50\%} = 400^\circ\text{C}$  and  $T_{90\%} > 550^\circ\text{C}$ ) than the reference catalyst and the beta-Co (HS). On the contrary, the Cu-exchanged zeolite beta showed a much better performance ( $T_{50\%} = 310^\circ\text{C}$  and  $T_{90\%} = 360^\circ\text{C}$ ) in the trichloroethylene oxidation than that achieved with the other zeolites, including the reference catalyst.

These results show that only the addition of copper by ion exchange can substantially improve the activity of the beta zeolite. This could be related with the physicochemical properties of this material that had together with a high acidity (indicated by the high ammonia adsorption), important redox properties, as it was reflected by the complete reduction of the copper species observed in the TPR experiments.

The results show that not only strong Brönsted acid sites can catalyze the TCE oxidation [18], but also metals with redox properties. In fact similar results were obtained with the H-beta, beta-Cu (HS), beta-Co (HS) and beta-Co (IE) catalysts in spite of their different acid properties. This indicates that in these samples, the oxidation of TCE was not necessarily catalyzed by the H-sites but by the copper and cobalt active sites, probably highly dispersed metallic clusters with some interaction with the zeolite framework. This is clearly evidenced by the similar light off curve obtained with beta-Co (HS) and beta-Co (IE) despite the different quantity of ammonia adsorbed by those zeolites (Table2).

These results also demonstrate that the interaction of the transition metal with the zeolite framework influences the catalytic activity. In this way, zeolites prepared by hydrothermal synthesis present lower activity than the ion exchanged zeolites probably because in the former ones small metal oxide particles are formed with much less interaction with the silicate framework, resulting in a lower redox activity than in the ion exchanged zeolites. Similar results have been described with this type of materials for other reactions [41, 42].

As it was suggested by other authors [18, 43], acidity also could play an important role in the catalyst activity as the best results were obtained with the catalyst with the highest ammonia

adsorption capacity and with the highest number of strong acid sites, i.e. the beta-Cu (IE). Nevertheless, this catalyst is also the one that was reduced at lower temperatures (**Figure 4**) and where the  $\text{Me}^{2+}$  was completely reduced (**Table 3**), being both results representative of its redox properties. This did not occur with the beta-Co (IE) zeolite that although had important acid properties, it had not important redox properties as it was reflected by the high temperature necessary for the partial reduction of the metal. For that reason this catalyst performed a lower catalyst activity if compared with the beta-Cu (IE) zeolite.

We propose that the combination of acid and redox properties is the key factor to design active catalysts in the TCE oxidation reaction. In this basis, we support the hypothesis that this reaction takes place in different steps [23, 44]: first the TCE molecule is adsorbed on the acid sites of the zeolite and then it reacts with the active oxygen species of the zeolite surface leading to the formation of reaction intermediates, which can be further oxidized in the presence of active oxygen species until being converted into  $\text{CO}_x$ , HCl,  $\text{Cl}_2$  and  $\text{H}_2\text{O}$ . In this way, a redox cycle occurs on the catalyst surface between the oxygen vacancies and the oxygen of the gas phase, and this determines both the activity and the selectivity of the reaction. Although the mechanism cannot be fully confirmed and *in situ* characterization experiments would be necessary to prove it, all the data obtained in this work point in this direction and thus, better acid and redox properties of the catalyst must result in a higher activity for the oxidation of the chloride species.

### 3.3. Product distribution

In all cases, the main oxidation products obtained in the trichloroethylene oxidation, when using the Cu and Co beta zeolites, were carbon dioxide ( $\text{CO}_2$ ) and hydrogen chloride (HCl). At mild temperatures, carbon monoxide (CO) and tetrachloroethylene ( $\text{C}_2\text{Cl}_4$ ) were also detected in the product stream. Chlorine ( $\text{Cl}_2$ ) was only detected at low concentration at temperatures above  $400^\circ\text{C}$ . **Figure 7** shows the product distribution in the TCE oxidation reaction over the most active catalyst studied in this work, the beta-Cu (IE).

As it can be seen, the selectivity towards  $\text{CO}_2$  of this catalyst was better than that obtained with other catalysts based on zeolites, where CO was the main carbon product formed [1, 45]. This can be related with the improved redox properties of this catalyst that favours the complete oxidation of the carbon species, especially at temperatures higher than  $500^\circ\text{C}$ . On the other hand HCl was the main chlorinated product obtained from the beginning of the reaction. The hydrogen atoms that are necessary to form the HCl molecule came both from the trichloroethylene molecules and from water impurities in the gas stream [15], although the H-Brönsted acid sites of the zeolite may also contribute to the formation of the HCl. On the other hand, a small amount of  $\text{C}_2\text{Cl}_4$  was detected

around 300-450°C, but at higher temperatures the concentration of this molecule decreases and it was completely decomposed at 550°C, temperature at which Cl<sub>2</sub> started to arise. This can be explained because at lower temperatures chloride molecules react with TCE to form tetrachloroethylene (C<sub>2</sub>Cl<sub>4</sub>). At higher temperatures when this by-product started to be destroyed, Cl<sub>2</sub> or/and metal chlorides could be formed, as it has been proposed by other authors [15, 46].

### 3.4. Catalyst stability

The stability of the catalysts was tested by using a Cu-zeolite that was previously used in a temperature transient experiment. The reaction was repeated with the used catalyst at 300°C during 70 hours. The results obtained with the beta-Cu (IE) zeolite are shown in **Figure 8**. The activity and selectivity of this catalyst remained almost constant at 300°C after 70 hours of reaction. The zeolite was characterized by XRD and BET (data not shown) after the stability test and no important changes were observed. These results are in contrast with those obtained when using H-zeolites [16, 47], where coke formation and chlorine attack causes the rapid deactivation of H-zeolites. It seems that the formation of coke in the strong Brönsted acid sites of beta-Cu (IE) zeolite was inhibited, due to the oxidative properties of the ion exchanged copper sites [32].

These results also show the advantage of using the zeolite catalysts instead of other catalysts based in metal oxides. Although some of them were more active [48, 49] and had shown a lower light off temperature, they could be quite unstable and they got deactivated due to the formation of Cl<sub>2</sub> or they could form some volatile and toxic subproducts [50, 51] that were not observed when using these zeolites.

## 4. CONCLUSIONS

In this work we studied for first time the catalytic activity for the TCE oxidation of different Cu and Co beta zeolites prepared by ion-exchange and by hydrothermal synthesis. The results show that all the materials are active catalysts for the TCE oxidation and that both the strong Brönsted acid sites and the copper and cobalt species can catalyze the TCE oxidation. Nevertheless, the preparation method has a significant role on the catalytic properties of the materials. The highest activity was obtained with the Cu-exchanged zeolite beta. This can be related with an optimum combination of acid and redox properties. These zeolites are more selective towards CO<sub>2</sub> than the acid zeolites previously described as active catalysts for this reaction. This can be connected to the oxidative properties of the copper exchanged sites that avoid the formation of coke in the strong acid sites of the zeolite. In this way these materials are more stable than the H-zeolites and they have not shown

any deactivation after 70 hours of reaction. On the other hand, the lower activity of the zeolites with Cu and Co prepared by hydrothermal synthesis can be attributed to the formation of small metal oxide particles with much less interaction with the silicate framework, resulting in a lower redox activity than in the ion exchanged zeolites. Thus, it can be concluded that an adequate combination of acidity, redox properties and metal-zeolite interaction is necessary in order to prepare an active catalyst for this reaction.

## ACKNOWLEDGEMENTS

The authors wish to thank the Spanish Ministry of Economy and Competitiveness through the MAT-2012-38567-C02-01 for the financial support. N.B.R. acknowledges Cátedra Cemex Sostenibilidad (UPV) for a fellowship.

## REFERENCES

- [1] J.R. Gonzalez-Velasco, A. Aranzabal, R. Lopez-Fonseca, R. Ferret, J.A. Gonzalez-Marcos, Enhancement of the catalytic oxidation of hydrogen-lean chlorinated VOCs in the presence of hydrogen-supplying compounds, *Appl. Catal.*, B 24 (2000) 33-43.
- [2] J. Caldwell, R. Lunn, A. Ruder, Trichloroethylene. IARC Monogr. Eval. Carcinog. Risks Hum., IARC (International Agency for Research on Cancer) 63 (1995) 75–158.
- [3] R.M. Heck, R.J. Farrauto, S.T. Gulati, *Catalytic Air Pollution Control. Commercial Technology*, Third ed., Hoboken, New Jersey, 2009.
- [4] S. Ojala, S. Pitkäaho, T. Laitinen, N. Niskala Koivikko, Catalysis in VOC abatement, *Topics in Catalysis* 54 (2011) 1224-1256.
- [5] L. Pinard, J. Mijoin, P. Ayrault, C. Canaff, P. Magnoux, On the mechanism of the catalytic destruction of dichloromethane over Pt zeolite catalysts, *Applied Catalysis B: environmental* 51 (2004) 1-8.
- [6] N. Blanch-Raga, A.E. Palomares, J. Martínez-Triguero, G. Fetter, P. Bosch, Cu Mixed Oxides Based on Hydrotalcite-Like Compounds for the Oxidation of Trichloroethylene, *Industrial & Engineering Chemistry Research* 52 (2013) 15772-15779.

- [7] N. Blanch-Raga, A.E. Palomares, J. Martínez-Triguero, M. Puche, G. Fetter, P. Bosch, The oxidation of trichloroethylene over different mixed oxides derived from hydrotalcites, *Applied Catalysis B: Environmental* 160–161 (2014) 129-134.
- [8] B. de Rivas, R. López-Fonseca, M.A. Gutiérrez-Ortiz, J.I. Gutiérrez-Ortiz, Impact of induced chlorine-poisoning on the catalytic behaviour of  $\text{Ce}_{0.5}\text{Zr}_{0.5}\text{O}_2$  and  $\text{Ce}_{0.15}\text{Zr}_{0.85}\text{O}_2$  in the gas-phase oxidation of chlorinated VOCs, *Applied Catalysis B: Environmental* 104 (2011) 373-381.
- [9] B. de Rivas, R. López-Fonseca, M.Á. Gutiérrez-Ortiz, J.I. Gutiérrez-Ortiz, Combustion of chlorinated VOCs using K-CeZrO<sub>4</sub> catalysts, *Catalysis Today* 176 (2011) 470-473.
- [10] B. de Rivas, R. López-Fonseca, C. Jiménez-González, J.I. Gutiérrez-Ortiz, Synthesis, characterisation and catalytic performance of nanocrystalline  $\text{Co}_3\text{O}_4$  for gas-phase chlorinated VOC abatement, *Journal of Catalysis* 281 (2011) 88-97.
- [11] G. Siquin, C. Petit, S. Libs, J.P. Hindermann, A. Kiennemann, Catalytic destruction of chlorinated C<sub>2</sub> compounds on a  $\text{LaMnO}_{3+\delta}$  perovskite catalyst, *Applied Catalysis B: Environmental* 32 (2001) 37-47.
- [12] N. Blanch-Raga, M.D. Soriano, A.E. Palomares, P. Concepción, J. Martínez-Triguero, J.M.L. Nieto, Catalytic abatement of trichloroethylene over Mo and/or W-based bronzes, *Applied Catalysis B: Environmental* 130–131 (2013) 36-43.
- [13] J. Corella, J.M. Toledo, A.M. Padilla, On the selection of the catalyst among the commercial platinum-based ones for total oxidation of some chlorinated hydrocarbons, *Applied Catalysis B: Environmental* 27 (2000) 243-256.
- [14] A. Aranzabal, B. Pereda-Ayo, M.P. González-Marcos, J. González-Marcos, R. López-Fonseca, J. González-Velasco, State of the art in catalytic oxidation of chlorinated volatile organic compounds, *Chemical Papers* 68 (2014) 1169-1186.
- [15] J.R. Gonzalez-Velasco, R. Lopez-Fonseca, A. Aranzabal, J.I. Gutierrez-Ortiz, P. Steltenpohl, Evaluation of H-type zeolites in the destructive oxidation of chlorinated volatile organic compounds, *Applied Catalysis B: Environmental* 24 (2000) 233-242.

- [16] A. Aranzabal, M. Romero-Sáez, U. Elizundia, J.R. González-Velasco, J.A. González-Marcos, Deactivation of H-zeolites during catalytic oxidation of trichloroethylene, *Journal of Catalysis* 296 (2012) 165-174.
- [17] R. Lopez-Fonseca, J.I. Gutierrez-Ortiz, M.A. Gutierrez-Ortiz, J.R. Gonzalez-Velasco, Dealuminated Y Zeolites for Destruction of Chlorinated Volatile Organic Compounds, *Jornal of Catalysis* 209 (2002) 145-150.
- [18] R. López-Fonseca, R.B. de, J.I. Gutierrez-Ortiz, A. Aranzabal, J.R. Gonzalez-Velasco, Enhanced activity of zeolites by chemical dealumination for chlorinated VOC abatement, *Applied Catalysis B: Environmental* 41 (2003) 31-42.
- [19] S. Chatterjee, H.L. Greene, Y.J. Park, Deactivation of metal exchanged zeolite catalysts during exposure to chlorinated hydrocarbons under oxidizing conditions, *Catalysis Today* 11 (1992) 569-596.
- [20] J.I. Gutierrez-Ortiz, R. Lopez-Fonseca, U. Aurrekoetxea, J.R. Gonzalez-Velasco, Low-temperature deep oxidation of dichloromethane and trichloroethylene by H-ZSM-5-supported manganese oxide catalysts, *J. Catal.* 218 (2003) 148-154.
- [21] A.Z. Abdullah, M.Z.A. Bakar, S. Bhatia, Combustion of chlorinated volatile organic compounds (VOCs) using bimetallic chromium-copper supported on modified H-ZSM-5 catalyst, *Journal of Hazardous Materials* 129 (2006) 39-49.
- [22] D. Divakar, M. Romero-Sáez, B. Pereda-Ayo, A. Aranzabal, J.A. González-Marcos, J.R. González-Velasco, Catalytic oxidation of trichloroethylene over Fe-zeolites, *Catalysis Today* 176 (2011) 357-360.
- [23] Q. Huang, Z. Meng, R. Zhou, The effect of synergy between  $\text{Cr}_2\text{O}_3$ - $\text{CeO}_2$  and USY zeolite on the catalytic performance and durability of chromium and cerium modified USY catalysts for decomposition of chlorinated volatile organic compounds, *Applied Catalysis B: Environmental* 115–116 (2012) 179-189.
- [24] A. Corma, L.T. Nemeth, M. Renz, S. Valencia, Sn-zeolite beta as a heterogeneous chemoselective catalyst for Baeyer-Villiger oxidations, *Nature* 412 (2001) 423-425.

- [25] Y. Zhu, G. Chuah, S. Jaenicke, Chemo- and regioselective Meerwein–Ponndorf–Verley and Oppenauer reactions catalyzed by Al-free Zr-zeolite beta, *Journal of Catalysis* 227 (2004) 1-10.
- [26] T. Blasco, M.A. Camblor, A. Corma, P. Esteve, J.M. Guil, A. Martínez, J.A. Perdigón-Melón, S. Valencia, Direct Synthesis and Characterization of Hydrophobic Aluminum-Free Ti–Beta Zeolite, *The Journal of Physical Chemistry B* 102 (1998) 75-88.
- [27] A. Corma, F.X. Llabrés i Xamena, C. Prestipino, M. Renz, S. Valencia, Water Resistant, Catalytically Active Nb and Ta Isolated Lewis Acid Sites, Homogeneously Distributed by Direct Synthesis in a Beta Zeolite, *The Journal of Physical Chemistry C* 113 (2009) 11306-11315.
- [28] M. Moreno-González, T. Blasco, K. Góra-Marek, A.E. Palomares, A. Corma, Study of propane oxidation on Cu-zeolite catalysts by in-situ EPR and IR spectroscopies, *Catalysis Today* 227 (2014) 123-129.
- [29] M.A. Camblor, A. Corma, S. Valencia, Spontaneous nucleation and growth of pure silica zeolite- $\beta$  free of connectivity defects, *Chemical Communications* (1996) 2365-2366.
- [30] L. Ren, L. Zhu, C. Yang, Y. Chen, Q. Sun, H. Zhang, C. Li, F. Nawaz, X. Meng, F.-S. Xiao, Designed copper-amine complex as an efficient template for one-pot synthesis of Cu-SSZ-13 zeolite with excellent activity for selective catalytic reduction of  $\text{NO}_x$  by  $\text{NH}_3$ , *Chemical Communications* 47 (2011) 9789-9791.
- [31] U. De La Torre, B. Pereda-Ayo, J.R. González-Velasco, Cu-zeolite  $\text{NH}_3$ -SCR catalysts for  $\text{NO}_x$  removal in the combined NSR–SCR technology, *Chemical Engineering Journal* 207–208 (2012) 10-17.
- [32] R. Bulánek, B. Wichterlová, Z. Sobalík, J. Tichý, Reducibility and oxidation activity of Cu ions in zeolites: Effect of Cu ion coordination and zeolite framework composition, *Applied Catalysis B: Environmental* 31 (2001) 13-25.
- [33] L. Capek, J. Dedecek, B. Wichterlová, L. Cider, E. Jobson, V. Tokarová, Cu-ZSM-5 zeolite highly active in reduction of NO with decane. Effect of zeolite structural parameters on the catalyst performance, *Applied Catalysis B: Environmental* 60 (2005) 147-153.



- [34] J. Sárkány, J.L. d'Itri, W.M.H. Sachtler, Redox chemistry in excessively ion-exchanged Cu/Na-ZSM-5, *Catalysis Letters* 16 (1992) 241-249
- [35] C. Franch-Martí, C. Alonso-Escobar, J.L. Jorda, I. Peral, J. Hernández-Fenollosa, A. Corma, A.E. Palomares, F. Rey, G. Guilera, TNU-9, a new zeolite for the selective catalytic reduction of NO: An in situ X-ray absorption spectroscopy study, *Journal of Catalysis* 295 (2012) 22-30.
- [36] J. Dedecek, D. Kaucký, B. Wichterlová, O. Gonsiorová, Co<sup>2+</sup> ions as probes of Al distribution in the framework of zeolites. ZSM-5 study, *Phys. Chem. Chem. Phys.* 4 (2002) 5406-5413.
- [37] L. Capek, J. Dedecek, P. Sazama, B. Wichterlová, The decisive role of the distribution of Al in the framework of beta zeolites on the structure and activity of Co ion species in propane-SCR-NO<sub>x</sub> in the presence of water vapour, *Journal of Catalysis* 272 (2010) 44-54.
- [38] E. M. Barea, V. Fornés, A. Corma, P. Bourges, E. Guillon, V. F. Puentes, A new synthetic route to produce metal zeolites with subnanometric magnetic clusters, *Chemical Communications* (2004) 1974-1975.
- [39] L. Capek, J. Dedecek, B. Wichterlová, Co-zeolite highly active in propane SCR- NO<sub>x</sub> in the presence of water vapour: effect of zeolite preparation and Al distribution in the framework, *Journal of Catalysis* 227 (2004) 352-366.
- [40] J. Dedecek, L. Capek, D. Kaucký, Z. Sobalík, B. Wichterlová, Siting and distribution of the Co ions in beta zeolite: A UV-Vis-NIR and FTIR study, *Journal of Catalysis* 211 (2002) 198-207.
- [41] A.E. Palomares, José G. Prato, F.E. Imbert, A.Corma, Catalysts based on tin and beta zeolite for the reduction of NO<sub>x</sub> under lean conditions in the presence of water, *Applied Catalysis B: Environmental* 75 (2007) 88-94.
- [42] A.E. Palomares, C. Franch, A.Corma, Determining the characteristics of a Co-zeolite to be active for the selective catalytic reduction of NO<sub>x</sub> with hydrocarbons, *Catalysis Today* 176 (2011) 239-241.

- [43] H. Valdés, V.A. Solar, E.H. Cabrera, A.F. Veloso, C.A. Zaror, Control of released volatile organic compounds from industrial facilities using natural and acid-treated mordenites: The role of acidic surface sites on the adsorption mechanism, *Chemical Engineering Journal* 244 (2014) 117-127.
- [44] J.I. Gutierrez-Ortiz, R.B. de, R. Lopez-Fonseca, J.R. Gonzalez-Velasco, Combustion of aliphatic C<sub>2</sub> chlorohydrocarbons over ceria-zirconia mixed oxides catalysts, *Applied Catalysis A* 269 (2004) 147-155.
- [45] S. Chatterjee, H.L. Greene, Effects of catalyst composition on dual site zeolite catalysts used in chlorinated hydrocarbon oxidation, *Applied Catalysis A: General* 98 (1993) 139-158.
- [46] J.C. Lou, S.S. Lee, Destruction of trichloromethane with catalytic oxidation, *Applied Catalysis B: environmental* 12 (1997) 111-123.
- [47] M. Gallastegi-Villa, A. Aranzabal, M. Romero-Sáez, J.A. González-Marcos, J.R. González-Velasco, Catalytic activity of regenerated catalyst after the oxidation of 1,2-dichloroethane and trichloroethylene, *Chemical Engineering Journal* 241 (2014) 200-206.
- [48] H. Li, G. Lu, Q. Dai, Y. Wang, Y. Guo, Y. Guo, Efficient low-temperature catalytic combustion of trichloroethylene over flower-like mesoporous Mn-doped CeO<sub>2</sub> microspheres, *Applied Catalysis B: environmental* 102 (2011) 475-483.
- [49] J. J. Spivey, Complete catalytic oxidation of volatile organics. *Ind. Eng. Chem. Res.* 26 (1987), 2165-2180.
- [50] A.M. Padilla, J. Corella, J.M. Toledo, Total oxidation of some chlorinated hydrocarbons with commercial chromia based catalysts. *Applied Catalysis B: environmental* 22 (1999) 107-121.
- [51] J.J. Spivey, J.B. Butt, Literature review: Deactivation of catalysts in the oxidation of volatile organic compounds. *Catalysis Today* 11 (1992) 465.

## **Caption to figures**

**Figure 1.** XRD patterns of H-beta, beta-Cu (IE), beta-Cu (HS), beta-Co (IE) and beta-Co (HS).

**Figure 2.** TEM images of beta-Cu zeolites prepared by ion exchange and by hydrothermal synthesis.

**Figure 3.** NH<sub>3</sub>-TPD profiles of beta-Cu (IE), beta-Cu (HS), beta-Co (IE) and beta-Co (HS).

**Figure 4.** TPR profiles of beta-Cu (IE), beta-Cu (HS), beta-Co (IE) and beta-Co (HS).

**Figure 5.** TCE conversion in a blank experiment, with a H-zeolite and over Cu and Co beta zeolites prepared by hydrothermal synthesis.

**Figure 6.** TCE conversion in a blank experiment, with a H-zeolite and over Cu and Co-exchanged beta zeolite.

**Figure 7.** Product distribution in the TCE oxidation reaction over beta-Cu (IE) zeolite.

**Figure 8.** TCE conversion over beta-Cu (IE) at 300°C for 70 hours.

**Table 1**

Catalyst	Molar ratio		Me <sup>2+</sup> (%wt)	% ion exchange	BET surface area (m <sup>2</sup> /g)	Mesopore volume (cm <sup>3</sup> /g)	Micropore volume (cm <sup>3</sup> /g)
	Si/Me <sup>2+</sup>	Si/Al					
H-beta	-	10.7	-	-	587	0.358	0.184
beta-Cu (IE)	31.6	10.8	3.16	68.4	572	0.359	0.175
beta-Co (IE)	40.0	10.7	1.97	53.3	586	0.381	0.178
beta-Cu (HS)	42.0	(without Al)	2.44	-	444	0.062	0.197
beta-Co (HS)	82.0	(without Al)	1.18	-	441	0.034	0.206

**Table 1.** Physico-chemical properties of the zeolite catalysts prepared by different methods. Me<sup>2+</sup> = Cu<sup>2+</sup> or Co<sup>2+</sup>

**Table 2**

<b>Catalyst</b>	<b>NH<sub>3</sub> (<math>\mu\text{mol}_{\text{NH}_3} \text{g}^{-1}</math>)</b>
beta-Cu (IE)	1606
beta-Co (IE)	1156
beta-Cu (HS)	78
beta-Co (HS)	47

**Table 2.** NH<sub>3</sub> desorbed per gram of zeolite in the NH<sub>3</sub>-TPD profiles.

**Table 3**

<b>Catalyst</b>	<b>H<sub>2</sub>-uptake (mmol H<sub>2</sub> g<sup>-1</sup>)</b>	<b>H<sub>2</sub>/(Cu or Co) molar ratio</b>
beta-Cu (IE)	0.58	≈ 1
beta-Co (IE)	0.19	0.57
beta-Cu (HS)	0.13	0.33
beta-Co (HS)	0.16	0.79

**Table 3.** H<sub>2</sub> uptake by the different catalysts in the TPR experiments.

Figure 1

Fig. 1

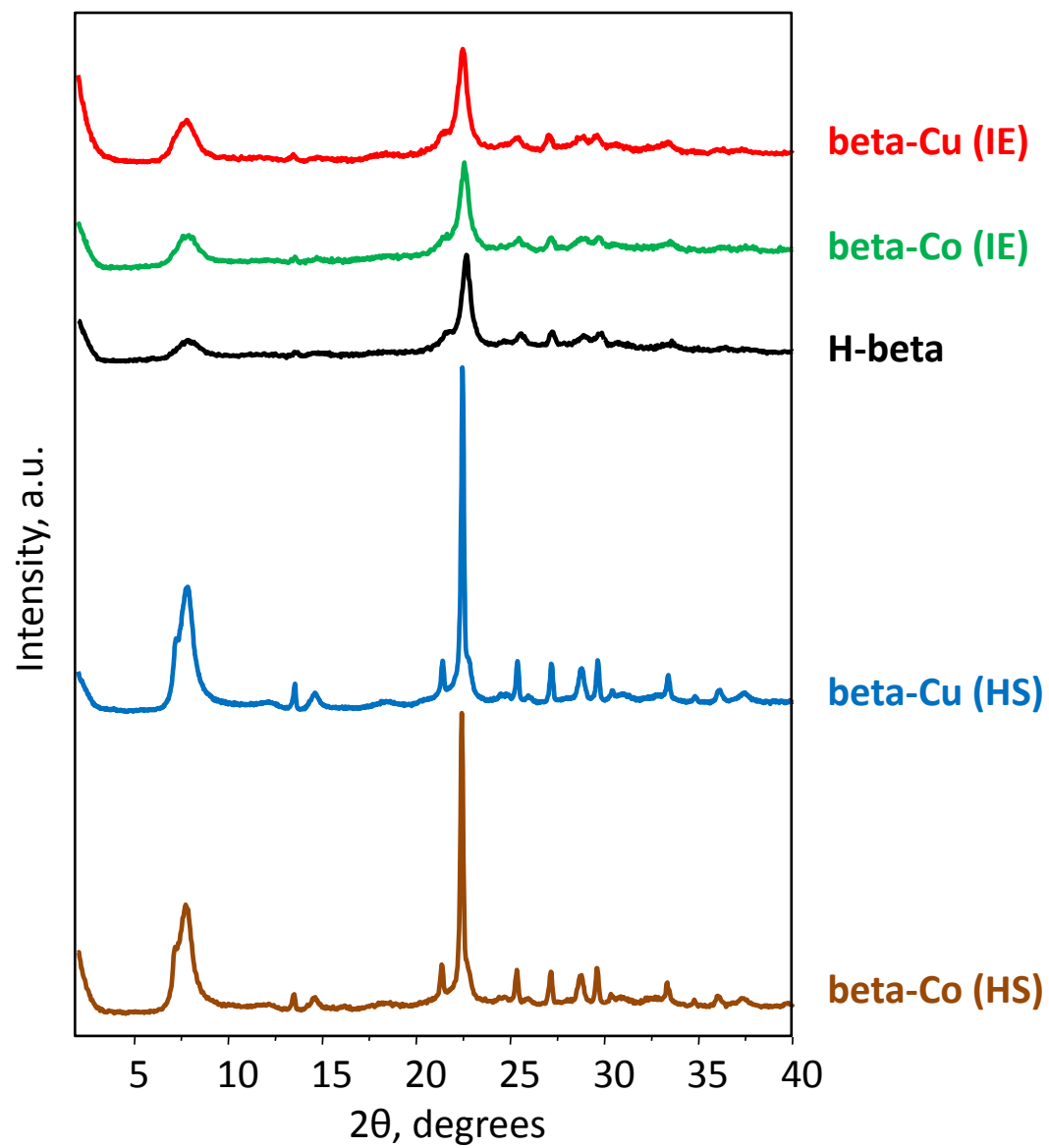
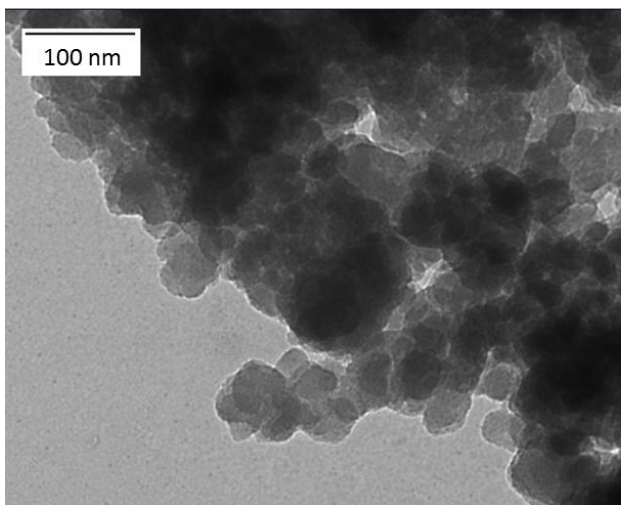
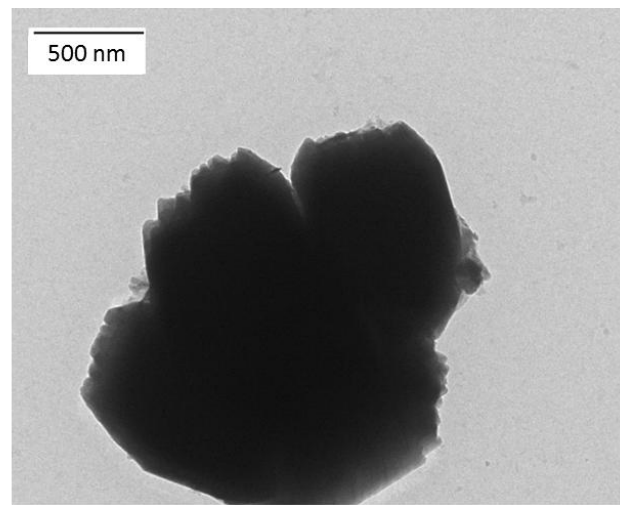


Fig. 2



Catalyst: beta-Cu (IE). (40000x)



Catalyst: beta-Cu (HS). (8000x)



Fig. 3

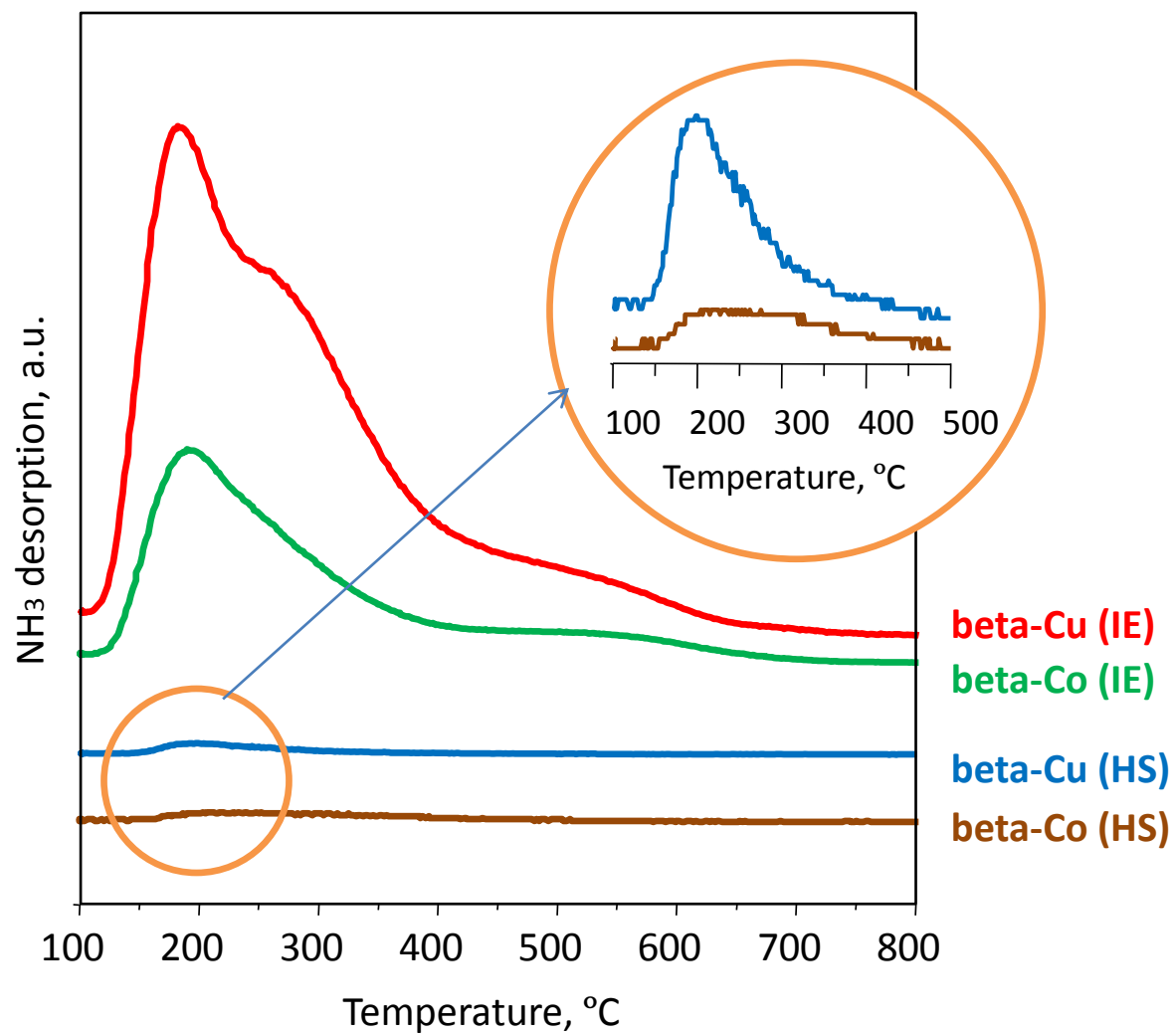


Figure 4

Fig. 4

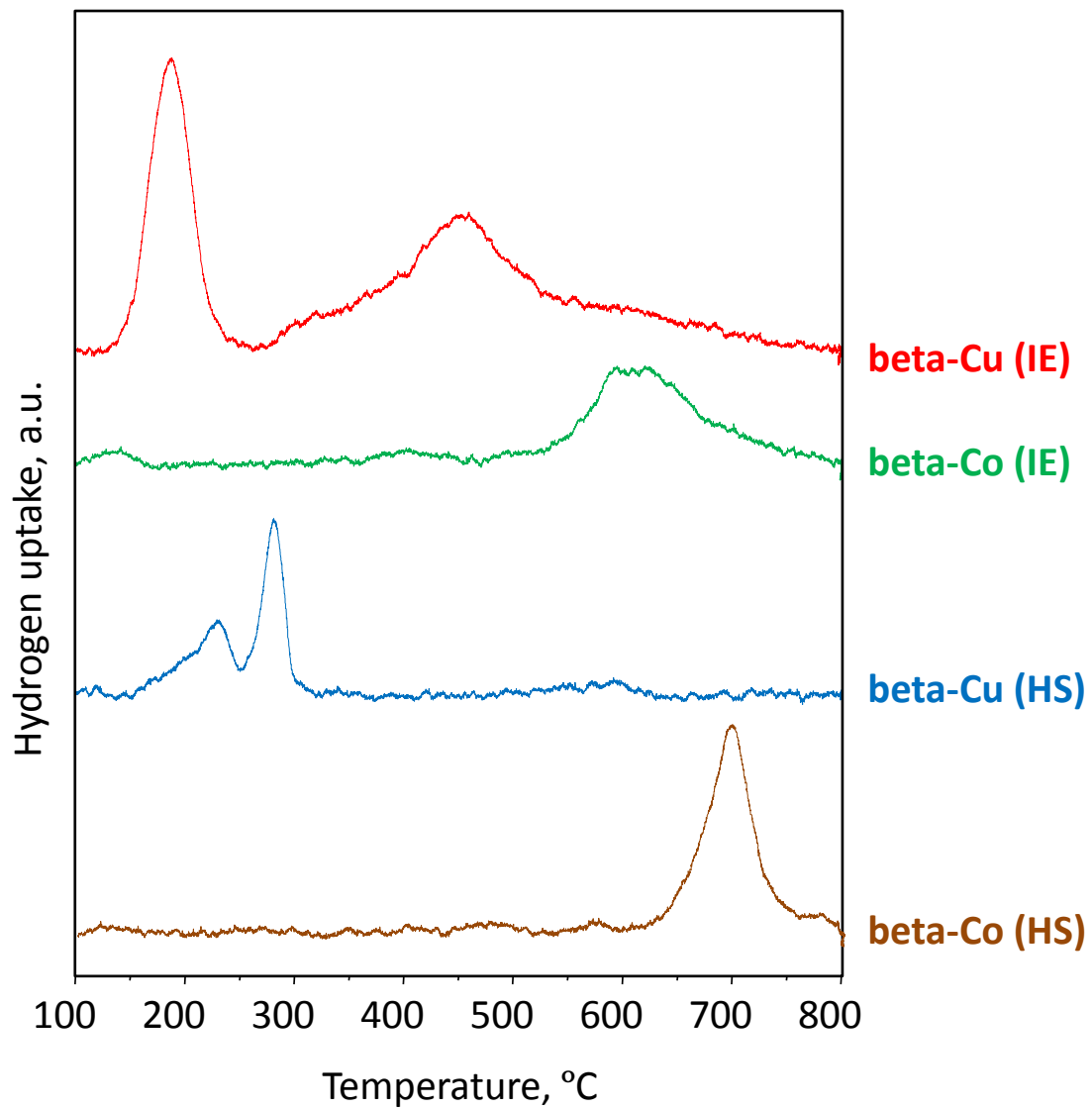


Figure 5

Fig. 5

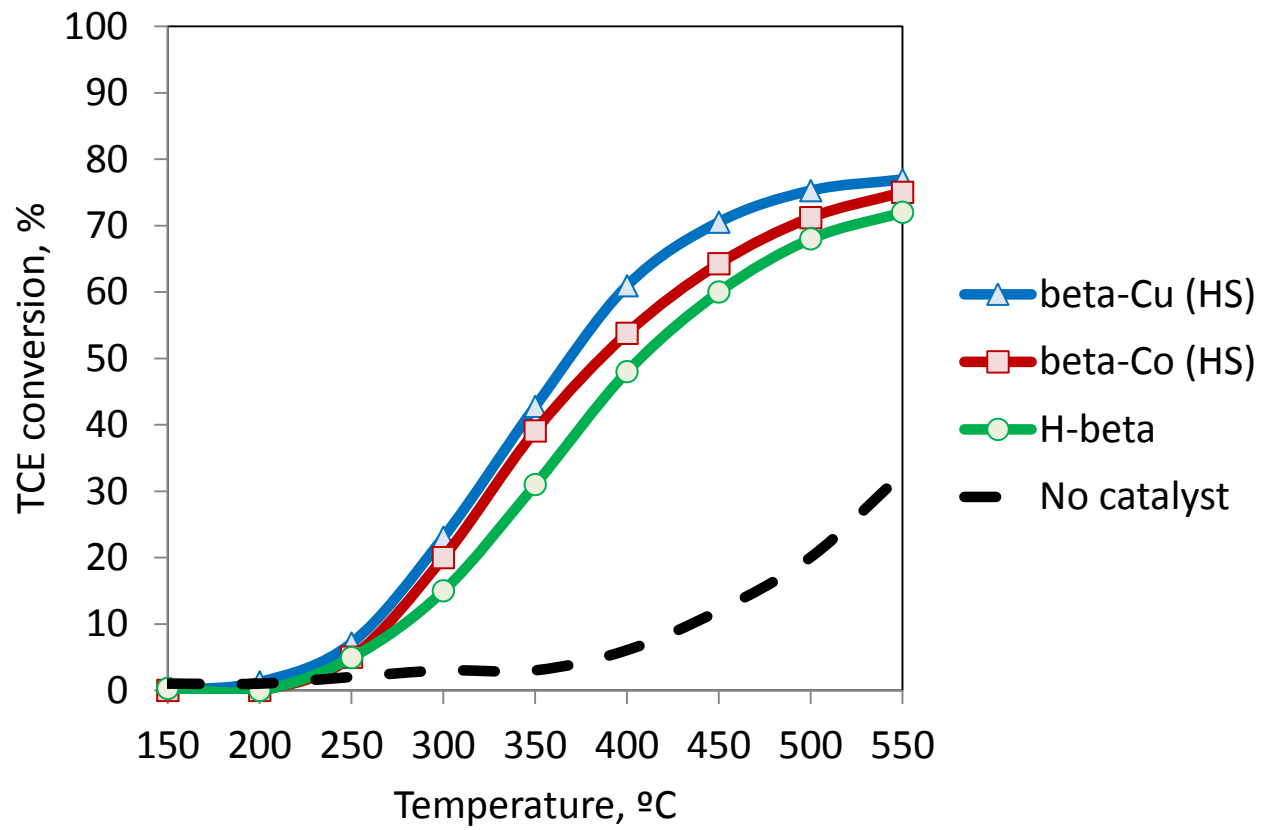


Fig. 6

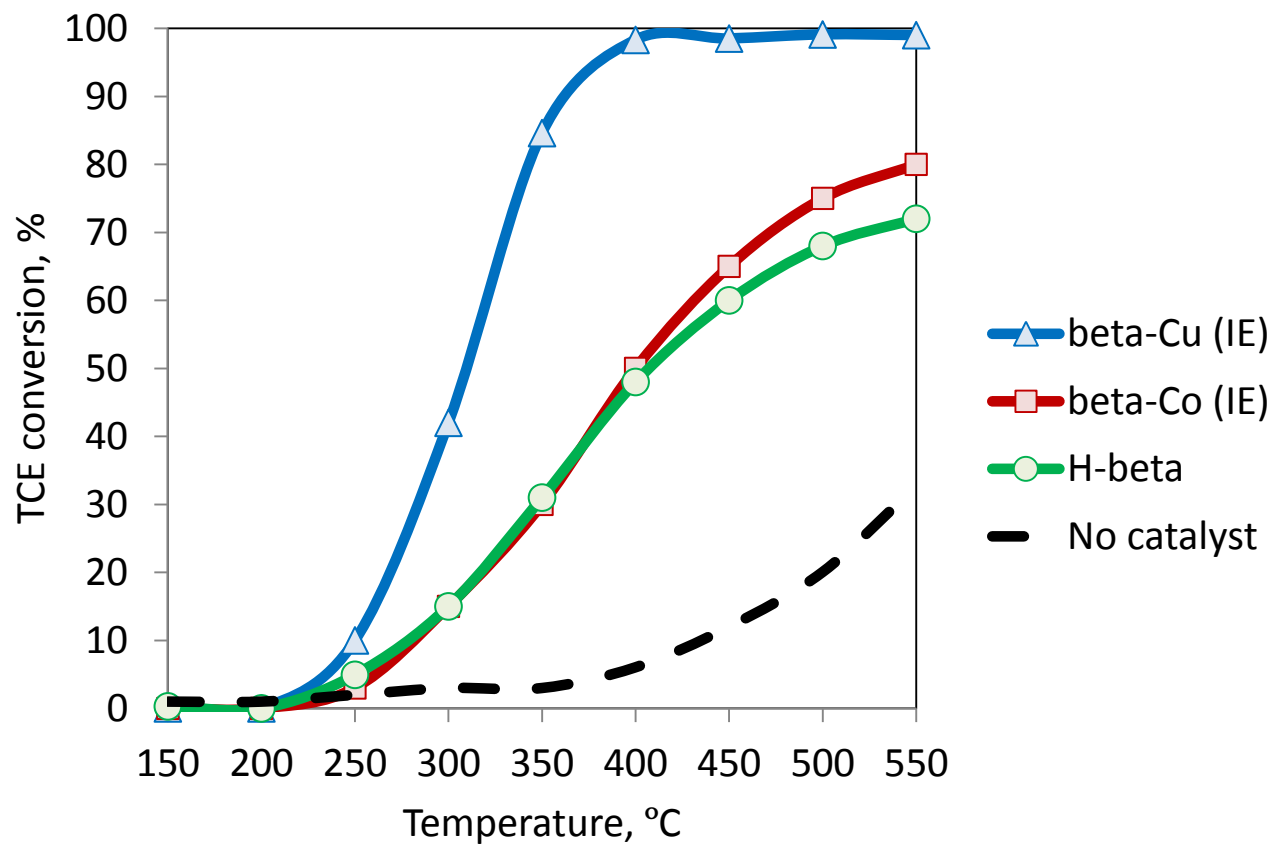


Figure 7

Fig. 7

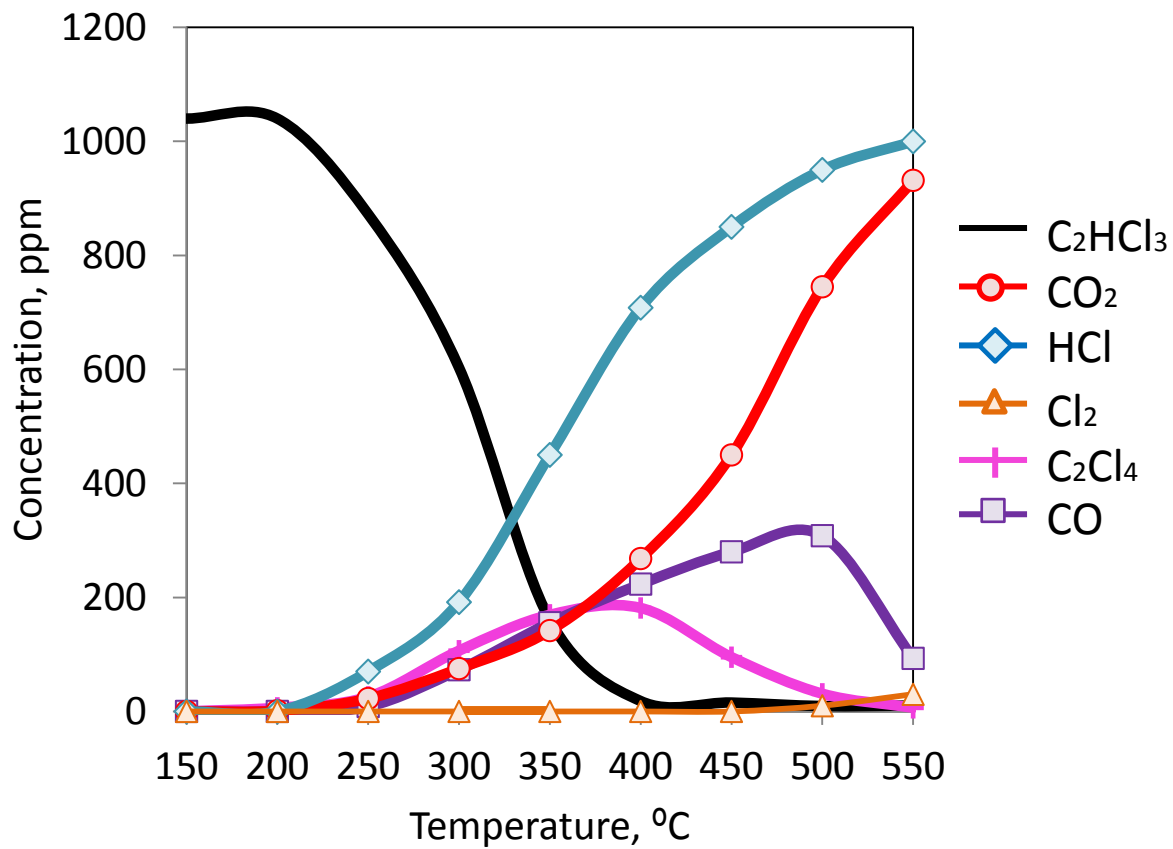


Figure 8

Fig. 8

